NACA

RESEARCH MEMORANDUM

INVESTIGATION OF THE AERODYNAMIC CHARACTERISTICS OF THE NACA RM-10 MISSILE (WITH FINS) AT A MACH NUMBER OF 1.62 IN THE LANGLEY 9-INCH SUPERSONIC TUNNEL

By Donald E. Coletti

Langley Aeronautical Laboratory
Langley Field, Va.

NATIONAL ADVISORY COMMITTEE
FOR AERONAUTICS
WASHINGTON

December 19, 1952
Declassified October 14, 1955

NATIONAL ADVISORY COMMITTEE FOR AERONAUTICS

RESEARCH MEMORANDUM

INVESTIGATION OF THE AERODYNAMIC CHARACTERISTICS OF THE NACA RM-10 MISSILE (WITH FINS) AT A MACH NUMBER OF 1.62 IN THE LANGLEY 9-INCH SUPERSONIC TUNNEL

By Donald E. Coletti

SUMMARY

An investigation has been made of a fin-stabilized 0.050-scale model of the NACA RM-10 missile at a Mach number of 1.62 and a Reynolds number of 2.66×10^6. Measurements were made of the lift, drag, and pitching moment of the finned body over an angle-of-attack range of $\pm 5^\circ$. Comparisons are made with results obtained from other test facilities.

The results show that changing the Reynolds number from 2.66×10^6 (the value used in the present investigation) to 29.2×10^6 (the value reported in NACA RM E50D28) has negligible effect upon the lift, pitching moment, and center-of-pressure position. The values of the various drag components of this investigation are in good agreement with those presented in NACA RM E50D28 and NACA RM L52A14 when proper consideration is given to the differences of Reynolds number. Increasing the ratio of sting-shield diameter to base diameter decreased the lift-curve slope, gave a less negative pitching-moment-curve slope, and decreased the fore drag at zero lift.

INTRODUCTION

As a part of a coordinated research program to evaluate scale effects at supersonic speeds, tests are being conducted at various NACA flight and wind-tunnel facilities on a slender parabolic body of revolution (with and without fins), designated as the NACA RM-10 missile. Results thus far obtained cover a wide range of model scale and Reynolds number within a Mach number range from approximately 1.5 to 3.5 (refs. 1 to 11). In general, correlation has been confined to the drag coefficient at zero lift.

The purpose of the tests reported in the present paper was to extend the investigation in the Langley 9-inch supersonic tunnel of the zero-lift drag components of the NACA RM-10 body alone (ref. 11) to include the effects of the fins on a 0.050-scale model, and to determine the lift, drag, and pitching moment of the finned body over an angle-of-attack range of $\pm 5^{\circ}$. The effects upon the aerodynamic characteristics of varying the ratio of sting-shield diameter to base diameter were also investigated. The tests were conducted at a Mach number of 1.62 and a Reynolds number of 2.66×10^{6}.

SYMBOLS

A maximum cross-section area of body

A_l wetted area of body forward of fin-body juncture

A_W wetted area of body alone (surface area forward of base)

α angle of attack of model

C_L lift coefficient, Lift/qA

C_D drag coefficient, Drag/qA

C_m pitching-moment coefficient about the station of maximum body diameter, Moment/qAL

$C_{L_\alpha} = \frac{dC_L}{d\alpha}$ at $C_L = 0$

$C_{m_\alpha} = \frac{dC_m}{d\alpha}$ at $C_L = 0$

d_b base diameter

d_{max} maximum body diameter

d_s sting-shield diameter at model base

L length of body

l distance from model nose to fin-body juncture

M Mach number

q dynamic pressure, $\rho V^2/2$

ρ stream density

r radius of body at an axial location

R Reynolds number, $\rho VL/\mu$

R_l Reynolds number based on distance l to fin-body juncture, $\rho V l/\mu$

V free-stream velocity

x axial distance from model nose

γ ratio of specific heats of air

θ cone angle of sting shield

μ coefficient of viscosity

Drag-coefficient subscripts:

B base drag

F fore drag (Total drag - Base drag)

f skin-friction drag

T total drag

W drag of four fins

w drag increment per fin

APPARATUS AND TESTS

Tunnel

The Langley 9-inch supersonic tunnel is a continuous-operation, closed-circuit type in which the pressure, temperature, and humidity of the enclosed air can be regulated. Different test Mach numbers are provided by interchangeable nozzle blocks which form test sections approximately 9 inches square. Eleven fine-mesh turbulence-damping screens are installed in the relatively large-area settling chamber ahead of the supersonic nozzle. Measurements of the longitudinal (stream direction) component of turbulence along the center line in the

entrance cone of the tunnel have indicated a root-mean-square value of approximately 0.14 percent (ref. 11). A schlieren optical system is provided for qualitative flow observations.

Model

A drawing of the 0.050-scale NACA RM-10 model, giving the pertinent dimensions, is shown in figure 1. The body has a parabolic-arc profile with a basic fineness ratio of 15. To facilitate rocket-motor installation in the free-flight missile, the rearward portion of the basic profile was removed, thus giving an actual fineness ratio of 12.2. Four stabilizing fins are attached 90° apart at the rear of the body. These fins have a 60° sweptback leading edge, a taper ratio of 1.0, and a 10-percent-thick circular-arc section normal to the leading edge.

Balance

The lift, drag, and pitching moment of the missile were measured by means of the tunnel's external self-balancing beam scales. The model was sting-mounted to the balance system and a sting shield extended up to the base of the model with a gap of approximately 0.004 inch. This sting shield was sealed to the balance housing by means of a rubber boot. For a more detailed description of the shield in relation to the body, see reference 12.

Tests, General

Tests were conducted at a Mach number of 1.62 and a Reynolds number of 2.66×10^{6} based on the body length. Measurements were made of lift, drag, and pitching moment about the station of maximum body diameter for an angle-of-attack range of $\pm 5^{\circ}$. Base-pressure measurements were obtained by the use of orifices located at the model base and in the balance housing. The values of base pressure at $\alpha = 0^{\circ}$ in this investigation are representative of free-flight base pressures (no sting) only when the effects due to the ratio of sting-shield diameter to base diameter are negligible. Because of the method of mounting the model and the unsymmetrical flow conditions at angles of attack not equal to 0°, the measured base pressure was not representative of flight base pressures. Therefore, the base pressures at $\alpha \neq 0^{\circ}$ were used only to obtain tare forces for evaluating missile fore drag (Total drag - Base drag).

The effect of support interference on the aerodynamic characteristics of the missile was investigated by means of three sting shields of varying

diameters. The geometric parameters are given in figure 1. The tests involving the two larger shields were made at various angles of attack, whereas the tests with the smallest shield were made only at an angle of attack of 0° because of the structural limitation of the model sting. The angle of attack was indicated by an optical system in conjunction with a small mirror mounted flush near the base of the body. The fins of the missile were inclined 45° to the plane of angle of attack.

Throughout the tests, the dew point was maintained below -20° F, where condensation effects are negligible.

CORRECTIONS AND ACCURACY

The accuracy of the free-stream Mach number is ±0.01 and represents a maximum variation about a mean Mach number throughout the test section. Corrections have been applied to the drag of the model at an angle of attack of 0° to account for the static-pressure variation along the tunnel center line. The same corrections were applied to the model at angles of attack. It is realized that the applications at $\alpha \neq 0^{\circ}$ are not strictly correct; however, the actual displacement of the model (from the tunnel center line) in traversing through its range of angles is small.

At $\alpha \neq 0^{\circ}$, the pressure at the model base was held approximately at free-stream static pressure by adjusting the pressure in the balance housing and, therefore, in the sting shield. The maximum deviation from this free-stream static pressure gave an error of ±0.0005 in C_{D_F}. This inaccuracy is a part of the total uncertainty. At $\alpha = 0^{\circ}$, a representative base pressure was obtained by varying the pressure in the balance housing so as to obtain a value of base pressure that corresponds to a condition of essentially no air flow through the sting shield.

The estimated accuracies of other test variables and the various coefficients are given below:

Reynolds number	$\pm 0.05 \times 10^6$
Initial angle of attack	±0.04°
Relative angle of attack	±0.01°
Lift coefficient	±0.0028
Pitching-moment coefficient	±0.0022
Fore drag coefficient	±0.0050
Base drag coefficient	±0.0010
Total drag coefficient	±0.0055

PRESENTATION AND DISCUSSION OF RESULTS

Variations Due to Angle of Attack

Lift, drag, and pitching moment.- The results of the measurements of the lift, fore drag, and pitching-moment coefficients, at angles of attack, of the fin-stabilized NACA RM-10 missile with two different sting shields are given in figures 2 and 3. The difference between the results for the two sting shields is the greater nonlinearity in the lift and pitching-moment coefficient curves at $\pm 2^{\circ}$ angle of attack for the configuration tested with the larger sting shield $\left(\frac{d_s}{d_b} = 0.99\right)$. The larger sting shield also gives a slightly less positive lift-curve slope at zero lift and a slightly less negative pitching-moment-curve slope. Also, the absolute value of the fore drag at any angle of attack is less for the larger sting shield. All of these differences may be attributed to the presence of the larger sting shield which creates higher pressures in the separated region over the lee side of the afterbody.

Center of pressure.- The variation of center-of-pressure position with angle of attack is shown in figure 4. The position is seen to be essentially constant for the higher angles of attack and is located at 10.4 body diameters behind the nose of the missile. These results are in good agreement with the data obtained from tests of a 0.050-scale model at the Lewis 8- by 6-foot supersonic tunnel (ref. 2) at a Reynolds number of 29.2×10^6, also shown in the figure. The location of the center of pressure obtained from tests of an 0.08-scale model at the Ames 1- by 3-foot supersonic tunnel (ref. 7) at a Mach number of 1.98 and Reynolds numbers of 8.6×10^6 and 17.4×10^6 is 10.3 diameters from the nose for all angles of attack, a value which is also in good agreement with the present results. Based on the results obtained in these three test facilities, there appears to be little or no effect upon the center-of-pressure position from Reynolds number or Mach number within the range of these investigations.

Comparisons of Lift, Drag, and Pitching Moment With Those From Other Facilities

Lift and pitching moment.- A comparison of the lift and pitching-moment coefficients of the present investigation with the results obtained in reference 2 is shown in figure 5. The results from reference 2 (Lewis 8- by 6-foot supersonic tunnel) were obtained at a Reynolds number of approximately 29.2×10^6 and at Mach numbers of 1.49,

1.59, 1.78, and 1.98. Inasmuch as the Reynolds number difference between the two investigations is large, the comparisons may be first-order only, because the flow over one model is essentially laminar while that over the other is for the most part turbulent. Nevertheless, the lift and pitching-moment data of the two facilities are in fair agreement.

It should be pointed out that whereas the results of the present investigation were obtained with the fins of the missile rolled 45° to the plane of angle of attack (fig. 1), the fins of the missile in reference 2 were parallel and normal to the plane of angle of attack. Spreiter has shown in reference 13 that linear theory predicts that the lift and pitching moment will be independent of the angle of roll at small angles of attack. This is verified by results presented in references 14 and 15 for different wing plan forms and roll angles. It is further shown in these two references that the drag is also independent of roll angle of the fins.

Drag.- A comparison of the fore drag coefficients of the various missile components at angles of attack with results from other facilities is shown in figure 6. The difference in the fore-drag results of the fin-body combination, at the smaller angles of attack, obtained in this investigation from that obtained in the Lewis 8- by 6-foot supersonic tunnel (ref. 2) is due primarily to the large difference in Reynolds number. The model tested in the present investigation has essentially laminar flow over the body upstream of the fins, whereas the model tested in the 8- by 6-foot supersonic tunnel has mostly turbulent flow, which results in considerably different skin-friction drags. Examples of the effects of Reynolds number on skin-friction drag for the RM-10 body may be seen in figure 18 of reference 11 or figure 8 of reference 9.

To obtain the drag of the four fins at angles of attack, it was necessary to resort to an indirect method since no angle-of-attack results were obtained with the body alone. The results of tests of a 0.29-scale model of the body alone in reference 8 (Langley 4- by 4-foot supersonic tunnel) were obtained at test conditions similar to those of the present investigation. As seen from figure 6, the value at 0° angle of attack is in fair agreement with that obtained in reference 11. The difference between the two values is perhaps due to the small variations in Mach number and Reynolds number of the two facilities. By assuming this difference to be constant over the range of angles investigated, values of fore drag were obtained for the body alone by adding this difference to the results from reference 8. It is realized that these values may not be strictly correct, but in view of the foregoing discussion they appear justifiable for the purpose of obtaining trends and orders of magnitude. The body-alone values thus obtained were then subtracted from the results for the fin-body

combination, at their respective angles of attack, to obtain the drag of the four fins. These values are shown in the right-hand portion of figure 6 and are compared with the results from reference 2. It should be pointed out that the drag coefficient of the four fins not only includes the pressure and skin-friction drags of the fins but also the interference between the fins plus the interference between the fins and body. In comparing the results obtained in the two facilities, it is seen that the drag of the fins obtained from the present investigation is slightly lower at angles of attack of 0° and 1° than the corresponding drags from reference 2, whereas the situation is reversed at angles above 1°. These differences may again be attributed mainly to the large difference in Reynolds number.

Effect of Variable Ratios of Sting-Shield Diameter to Base Diameter on the Drag Coefficients

The variation of the drag coefficients with different ratios of sting-shield diameter to base diameter d_s/d_b at 0° angle of attack is shown in figure 7.

Total drag.- The values obtained for the total drag of the fin-body combination in the present investigation with the two different sting-shield diameters $\left(\frac{d_s}{d_b} = 0.49 \text{ and } 0.72\right)$ are very nearly the same. No values of total drag and base drag were obtained for the missile with the ratio of $\frac{d_s}{d_b} = 0.99$, since the pressure at the model base was maintained at approximately free-stream static pressure. A comparison of these values of total drag for the fin-body combination with the value obtained from reference 8 shows very good agreement. The value obtained from reference 2 is considerably higher than these results, primarily because of the greater extent of turbulent boundary layer at the higher test Reynolds number. The same comparisons may be applied to the body-alone results obtained from references 2, 8, and 11.

Base drag.- The two base-drag results for the fin-body combination obtained in the present investigation are essentially independent of d_s/d_b. Comparison of these results with those obtained in references 2 and 8 shows them to be in very good agreement. This agreement is due, in all probability, to the fin-body juncture, which causes transition from a laminar to a turbulent boundary layer over the rear portion of the body. As shown in reference 11, when the flow is turbulent the base drag is very nearly constant, regardless of Reynolds number. The body-alone result obtained from reference 2 agrees very closely with the

value for the fin-body combination. This agreement and that shown in the preceding comparison indicate that in this Mach number range the effects of the fins upon the base pressure are for the most part eliminated when the Reynolds number exceeds that for natural transition on the body alone; this Reynolds number was shown in reference 11 to be near 9×10^6 at a Mach number of 1.62. The base-drag values of the body alone obtained from references 8 and 11 are in excellent agreement regardless of the different ratios of d_s/d_b.

Fore drag.- As shown in figure 7, varying the ratios of d_s/d_b from 0.49 to 0.72 has no effect on the fore drag of the fin-body combination in the present investigation. However, when d_s/d_b is equal to 0.99 the value of fore drag is reduced approximately 10 percent. Recent schlieren photographs, obtained in the 9-inch supersonic tunnel, of a fin-stabilized parabolic body of revolution with varying ratios of d_s/d_b (ref. 16) show that when the sting-shield diameter is considerably less than the base diameter, the flow is allowed to continue its expansion beyond the base of the model before reaching the sting. At this point, the flow must turn through an angle to be parallel to the sting, consequently producing a trailing shock. When the ratio of d_s/d_b is increased to 0.99, the shock moves forward to the base of the model. The presence of the trailing shock at the model base causes separation forward of the base and allows the higher-pressure air behind the shock to flow forward into the dead-air region and boundary layer, thus reducing the over-all fore drag.

The solid line on figure 7 represents a theoretical estimate of the fore drag of the fin-body combination at a Mach number of 1.62 and a Reynolds number of 2.66×10^6. This theoretical fore-drag estimate is the summation of the pressure drag of the body alone, the skin-friction drag of the body alone, the fin pressure drag, and the fin skin-friction drag. No calculations were made of interference arising between the fins and body. The equations used in the calculation of the body fore drag were based on the conclusions reached in reference 11, which states that the method of Lighthill (ref. 17) and the method of Jones and Margolis (ref. 18) gave a fair prediction of the pressure drag, that the Blasius incompressible theory gave a satisfactory prediction of the laminar skin-friction drag, and that the Frankl-Voishel extended theory (ref. 19) gave a reasonable prediction of the turbulent skin-friction drag. The theoretical pressure drag used in the calculation of the fore drag of the fin-body combination has therefore been taken as the average of the results obtained by the method of Lighthill and the method of Jones and Margolis. The skin-friction drag of the body alone was obtained by assuming that the flow over the body forward of the fin-body juncture was laminar and that behind this juncture the flow was turbulent. The Blasius incompressible theory for laminar skin-friction drag and the

Frankl-Voishel extended theory for turbulent skin-friction drag were combined to obtain the total skin-friction drag of the body in the following equation:

$$C_{D_f} = \frac{1.328}{\sqrt{R_l}} \frac{A_l}{A} + \frac{0.074}{\sqrt[5]{R}} \left(\frac{1}{1 + \frac{\gamma - 1}{2} M^2}\right)^{0.467} \frac{A_w - A_l}{A} \qquad (1)$$

The pressure drag of the fins was computed by the method of reference 20, and the fin skin-friction drag was computed by the Blasius incompressible theory for laminar flow. This estimate of the fore drag of the fin-body combination is in fair agreement with the results obtained in the present investigation.

The value of fore drag for the fin-body combination obtained from reference 8 is in excellent agreement with the results of this investigation. However, the value obtained from reference 2 is considerably higher than these results because of the higher skin-friction drag resulting from the greater regions of turbulent boundary layer. The fore-drag results obtained from references 2, 8, and 11 for the body alone indicate the same trends as the fore-drag results for the fin-body combination. The dashed line on figure 7 represents the extrapolated experimental fore drag of the body alone at a Mach number of 1.62 and a Reynolds number of 30×10^6, obtained from reference 11. This drag value is in fair agreement with that obtained from reference 2.

Drag per fin.- In figure 7 all of the drag-per-fin results obtained in the present investigation and those from references 2 and 8 are in excellent agreement regardless of the different values of d_s/d_b. The values of fore drag for the fins in this investigation were obtained as the difference between the fore drag of the fin-body combination and that of the body alone. Also shown on this figure is a theoretical drag estimate for one fin at a Mach number of 1.62 and a Reynolds number of 2.66×10^6. The equations used in this computation were the same as those used in obtaining the theoretical fore drag of the fin-body combination. It should again be pointed out that the experimental results include any interference arising between the fins and body, while the theoretical estimate of fin drag includes only the summation of the pressure drag and laminar skin-friction drag. This prediction of drag per fin is in excellent agreement with the experimental results.

CONCLUSIONS

An investigation has been made in the Langley 9-inch supersonic tunnel of a fin-stabilized 0.050-scale model of the NACA RM-10 missile

at a Mach number of 1.62 and a Reynolds number of 2.66×10^6. Measurements were made of the lift, drag, and pitching moment over an angle-of-attack range of $\pm 5^\circ$, and comparisons were made with similar results obtained in other test facilities. The effect of varying the ratio of sting-shield diameter to base diameter on the aerodynamic characteristics was also investigated. The following conclusions are indicated.

1. Comparison of the results of this investigation with results presented in NACA RM E50D28 (0.50-scale model) shows that changing the Reynolds number from 2.66×10^6 to 29.2×10^6 has no appreciable effect on the values of the lift and pitching-moment coefficients.

2. The center-of-pressure position is essentially constant over the angle-of-attack range of this investigation. A comparison of the present results with those reported in NACA RM E50D28 (0.50-scale model) and NACA RM A51G13 (0.08-scale model) indicates that little or no change of position due to model scale occurs within the Mach number and Reynolds number range of these investigations.

3. With proper consideration of Reynolds number, there is good agreement of the various drag components (total, base, and fore drag of the complete configuration and the drag per fin) with the results reported in NACA RM E50D28 (0.50-scale model) and NACA RM L52A14 (0.29-scale model) at 0° angle of attack.

4. Increasing the ratio of sting-shield diameter to base diameter decreased the lift-curve slope, gave a less negative pitching-moment-curve slope, and decreased the fore drag at zero lift.

Langley Aeronautical Laboratory,
National Advisory Committee for Aeronautics,
Langley Field, Va.

REFERENCES

1. Luidens, Roger W., and Simon, Paul C.: Aerodynamic Characteristics of NACA RM-10 Missile in 8- by 6-Foot Supersonic Wind Tunnel at Mach Numbers From 1.49 to 1.98. I - Presentation and Analysis of Pressure Measurements (Stabilizing Fins Removed). NACA RM E50D10, 1950.

2. Esenwein, Fred T., Obery, Leonard J., and Schueller, Carl F.: Aerodynamic Characteristics of NACA RM-10 Missile in 8- by 6-Foot Supersonic Wind Tunnel at Mach Numbers From 1.49 to 1.98. II - Presentation and Analysis of Force Measurements. NACA RM E50D28, 1950.

3. Luidens, Roger W., and Simon, Paul C.: Aerodynamic Characteristics of NACA RM-10 Missile in 8- by 6-Foot Supersonic Wind Tunnel at Mach Numbers from 1.49 to 1.98. III - Analysis of Force Distribution at Angle of Attack (Stabilizing Fins Removed). NACA RM E50I19, 1950.

4. Jackson, H. Herbert, Rumsey, Charles B., and Chauvin, Leo T.: Flight Measurements of Drag and Base Pressure of a Fin-Stabilized Parabolic Body of Revolution (NACA RM-10) at Different Reynolds Numbers and at Mach Numbers from 0.9 to 3.3. NACA RM L50G24, 1950.

5. Chauvin, Leo T., and deMoraes, Carlos A.: Correlation of Supersonic Convective Heat-Transfer Coefficients From Measurements of the Skin Temperature of a Parabolic Body of Revolution (NACA RM-10). NACA RM L51A18, 1951.

6. Rumsey, Charles B., and Loposer, J. Dan: Average Skin-Friction Coefficients From Boundary-Layer Measurements in Flight on a Parabolic Body of Revolution (NACA RM-10) at Supersonic Speeds and at Large Reynolds Numbers. NACA RM L51B12, 1951.

7. Perkins, Edward W., Gowen, Forrest E., and Jorgensen, Leland H.: Aerodynamic Characteristics of the NACA RM-10 Research Missile in the Ames 1- by 3-Foot Supersonic Wind Tunnel No. 2 - Pressure and Force Measurements at Mach Numbers of 1.52 and 1.98. NACA RM A51G13, 1951.

8. Hasel, Lowell E., Sinclair, Archibald R., and Hamilton, Clyde V.: Preliminary Investigation of the Drag Characteristics of the NACA RM-10 Missile at Mach Numbers of 1.40 and 1.59 in the Langley 4- by 4-Foot Supersonic Tunnel. NACA RM L52A14, 1952.

9. Czarnecki, K. R., and Marte, Jack E.: Skin-Friction Drag and Boundary-Layer Transition on a Parabolic Body of Revolution (NACA RM-10) at a Mach Number of 1.6 in the Langley 4- by 4-Foot Supersonic Pressure Tunnel. NACA RM L52C24, 1952.

10. Czarnecki, K. R., and Sinclair, Archibald R.: Preliminary Investigation of the Effects of Heat Transfer on Boundary-Layer Transition on a Parabolic Body of Revolution (NACA RM-10) at a Mach Number of 1.61. NACA RM L52E29a, 1952.

11. Love, Eugene S., Coletti, Donald E., and Bromm, August F.: Investigation of the Variation With Reynolds Number of the Base, Wave, and Skin-Friction Drag of a Parabolic Body of Revolution (NACA RM-10) at Mach Numbers of 1.62, 1.93, and 2.41 in the Langley 9-Inch Supersonic Tunnel. NACA RM L52H21, 1952.

12. Rainey, Robert W.: Langley 9-Inch Supersonic Tunnel Tests of Several Modifications of a Supersonic Missile Having Tandem Cruciform Lifting Surfaces. Three-Component Data Results of Models Having Ratios of Wing Span to Tail Span Equal to 1. NACA RM L9L30, 1951.

13. Spreiter, John R.: The Aerodynamic Forces on Slender Plane- and Cruciform-Wing and Body Combinations. NACA Rep. 962, 1950 (Supersedes NACA TN's 1897 and 1662.)

14. Grigsby, Carl E.: Tests at Mach Number 1.62 of a Series of Missile Configurations Having Tandem Cruciform Lifting Surfaces. NACA RM L51J15, 1952.

15. Rainey, Robert W.: An Investigation of Several Supersonic Missile Configurations Directed Toward Minimizing Center-of-Pressure Travel. NACA RM L52G01, 1952.

16. Love, Eugene S., and O'Donnell, Robert M.: Investigations at Supersonic Speeds of the Base Pressure on Bodies of Revolution With and Without Sweptback Stabilizing Fins. NACA RM L52J21a, 1952.

17. Lighthill, M. J.: Supersonic Flow Past Bodies of Revolution. R. & M. No. 2003, British A.R.C., 1945.

18. Jones, Robert T., and Margolis, Kenneth: Flow Over a Slender Body of Revolution at Supersonic Velocities. NACA TN 1081, 1946.

19. Rubesin, Morris W., Maydew, Randall C., and Varga, Steven A.: An Analytical and Experimental Investigation of the Skin Friction of the Turbulent Boundary Layer on a Flat Plate at Supersonic Speeds. NACA TN 2305, 1951.

20. Harmon, Sidney M., and Swanson, Margaret D.: Calculations of the Supersonic Wave Drag of Nonlifting Wings With Arbitrary Sweepback and Aspect Ratio. Wings Swept Behind the Mach Lines. NACA TN 1319, 1947.

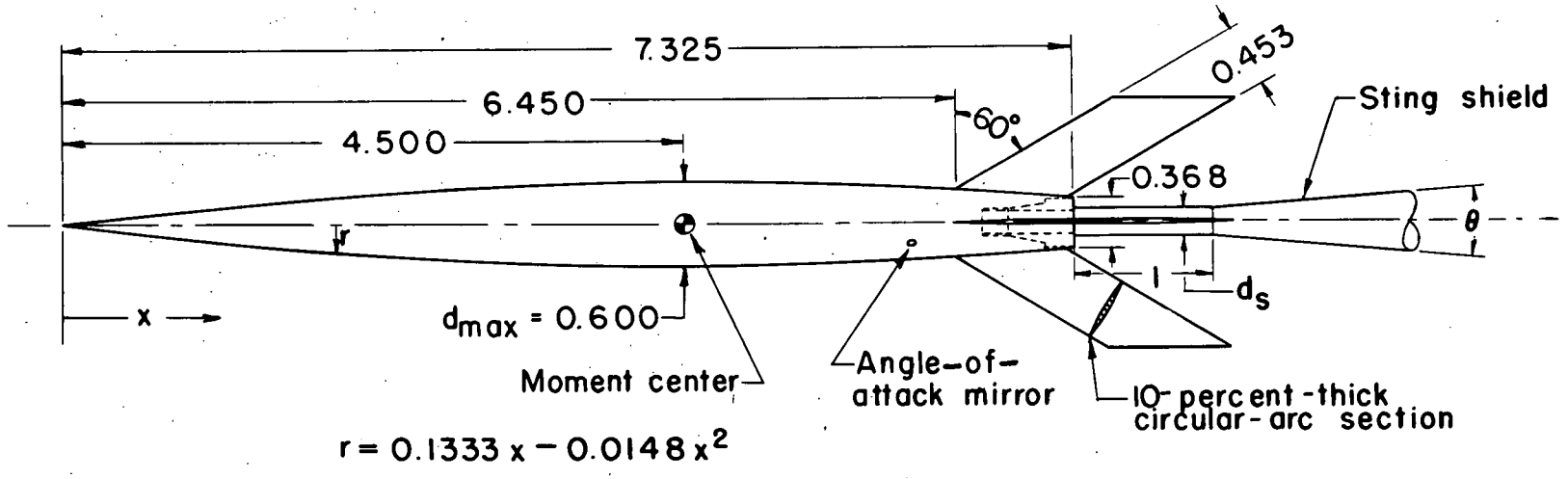

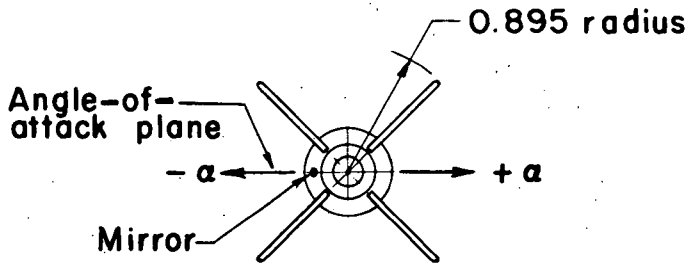

Sting shield	
d_s	θ, deg
0.180	14.5
0.263	13
0.365	11

Figure 1.- Drawing of 0.050-scale model of NACA RM-10 missile. All linear dimensions are in inches.

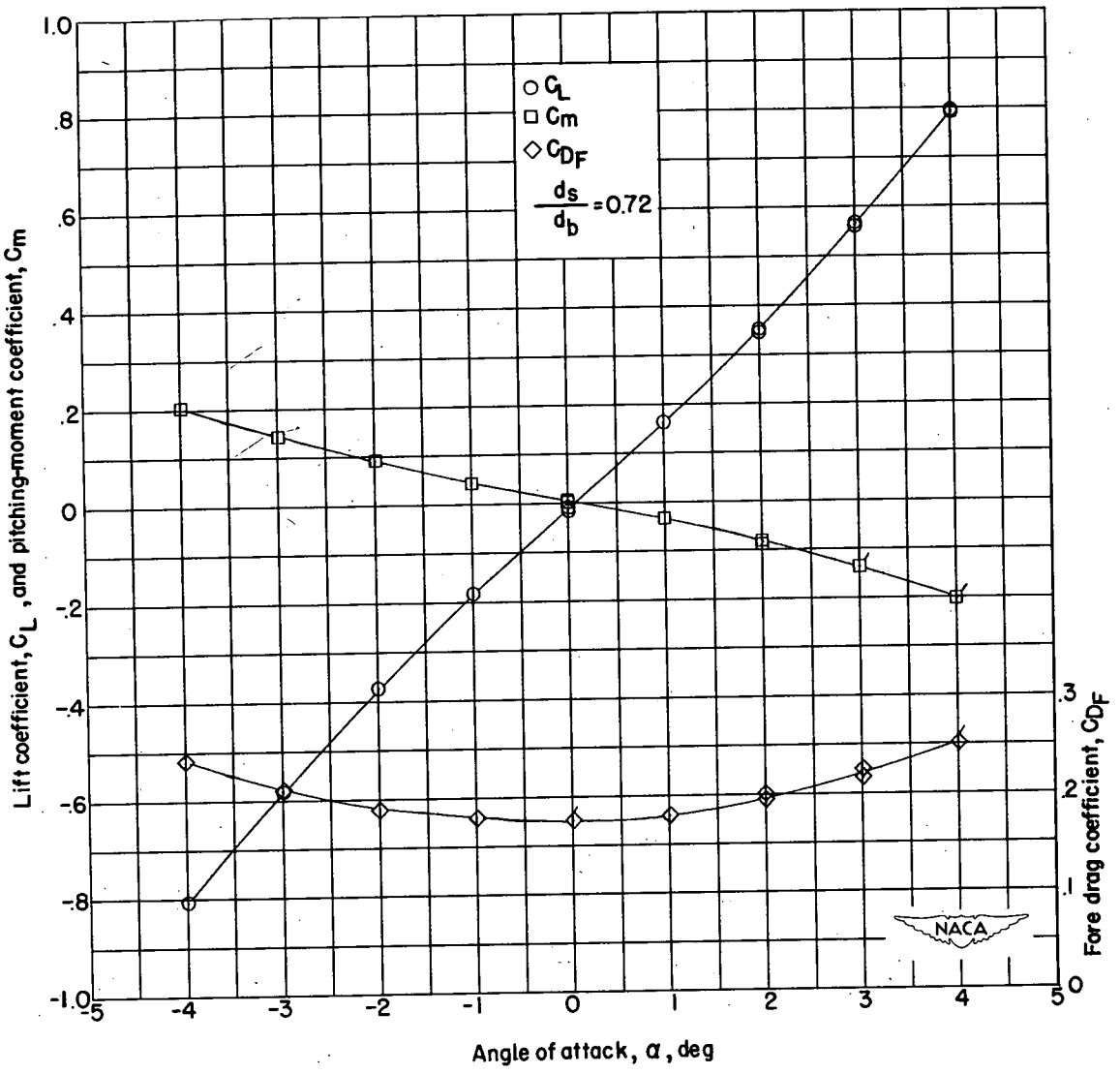

Figure 2.- Aerodynamic characteristics of the fin-stabilized NACA RM-10 missile with the ratio of sting-shield diameter to base diameter of 0.72 at a Mach number of 1.62 and a Reynolds number of 2.66×10^6. Flagged symbols denote check values.

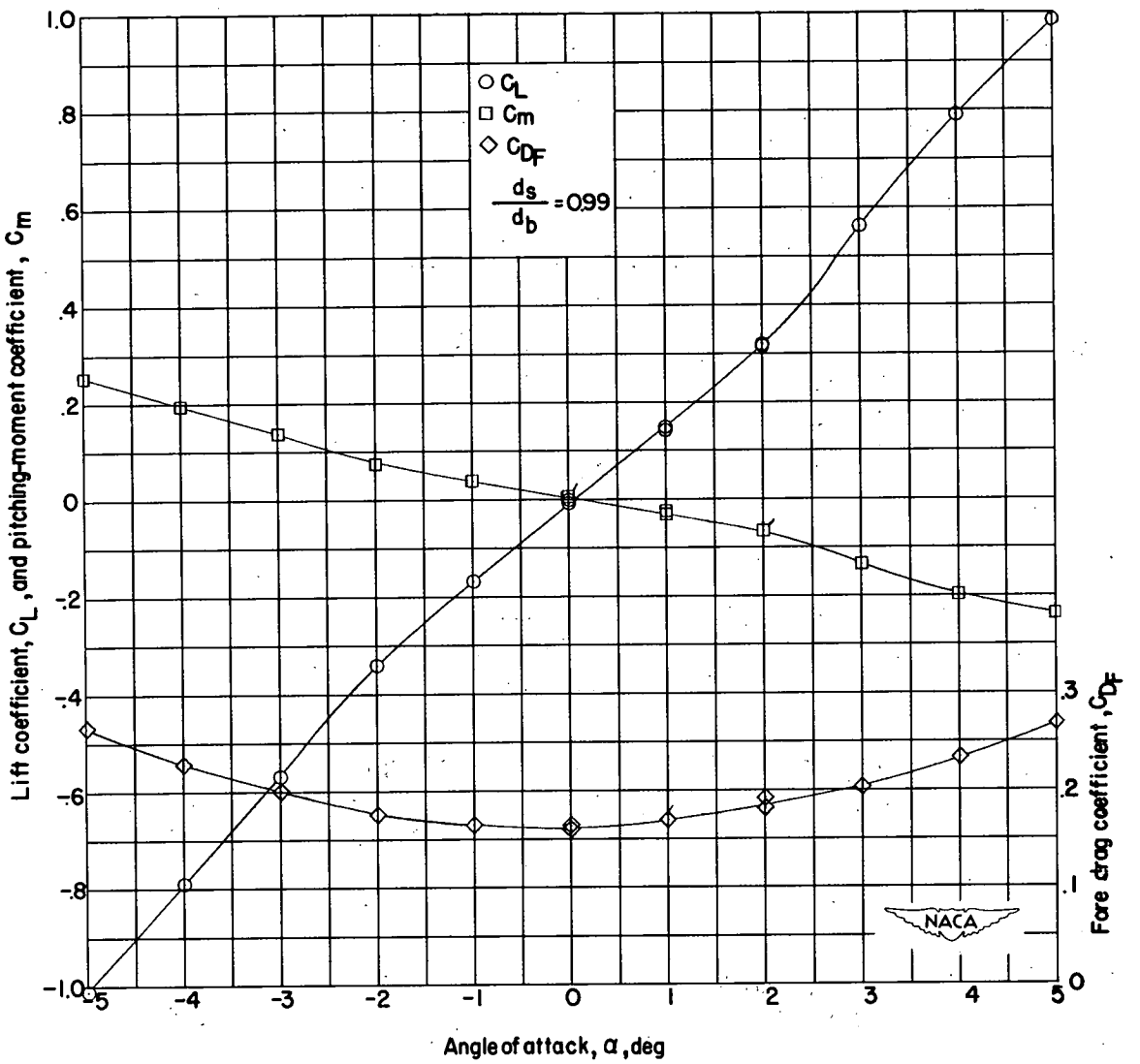

Figure 3.- Aerodynamic characteristics of the fin-stabilized NACA RM-10 missile with the ratio of sting-shield diameter to base diameter of 0.99 at a Mach number of 1.62 and a Reynolds number of 2.66×10^6. Flagged symbols denote check values.

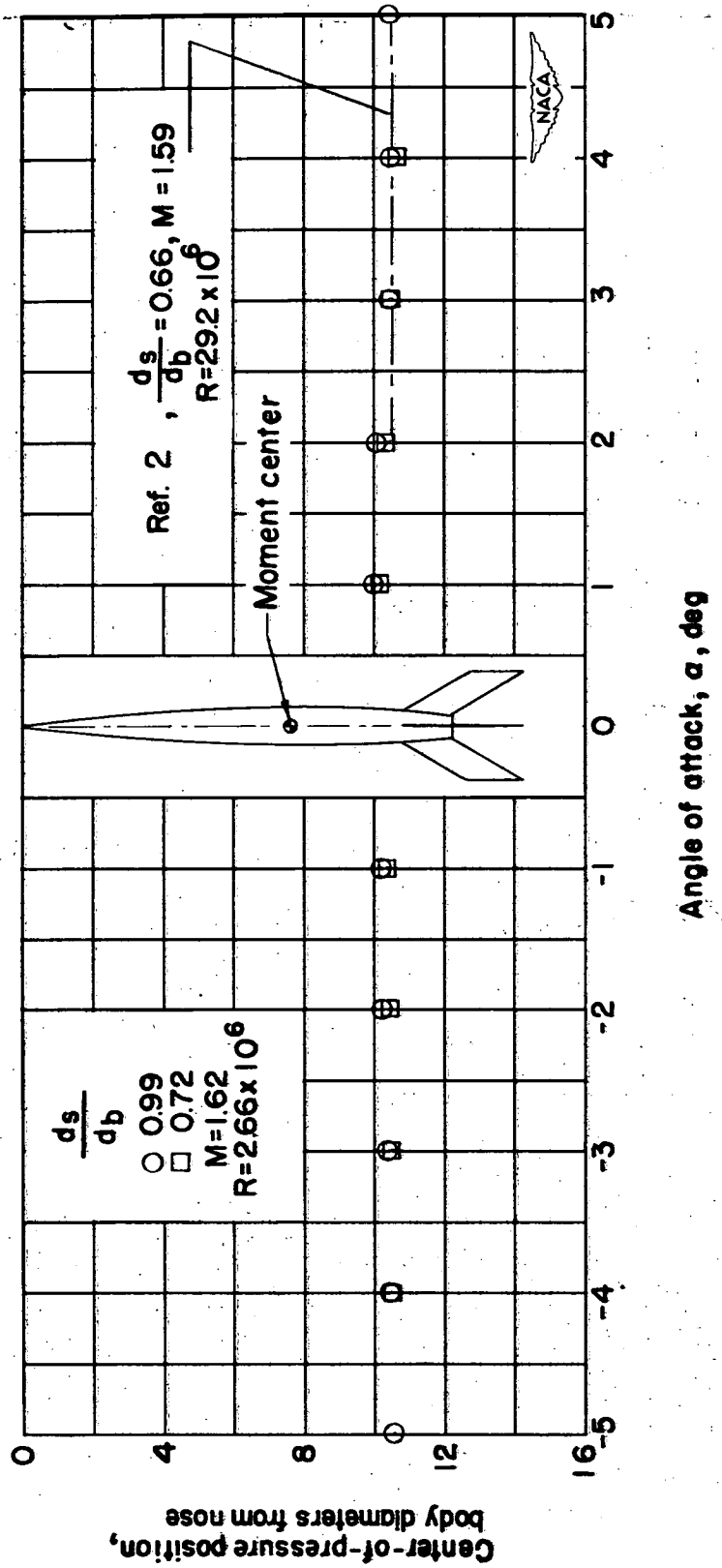

Figure 4.- Variation of center-of-pressure position with angle of attack at a Mach number of 1.62 and a Reynolds number of 2.66×10^6.

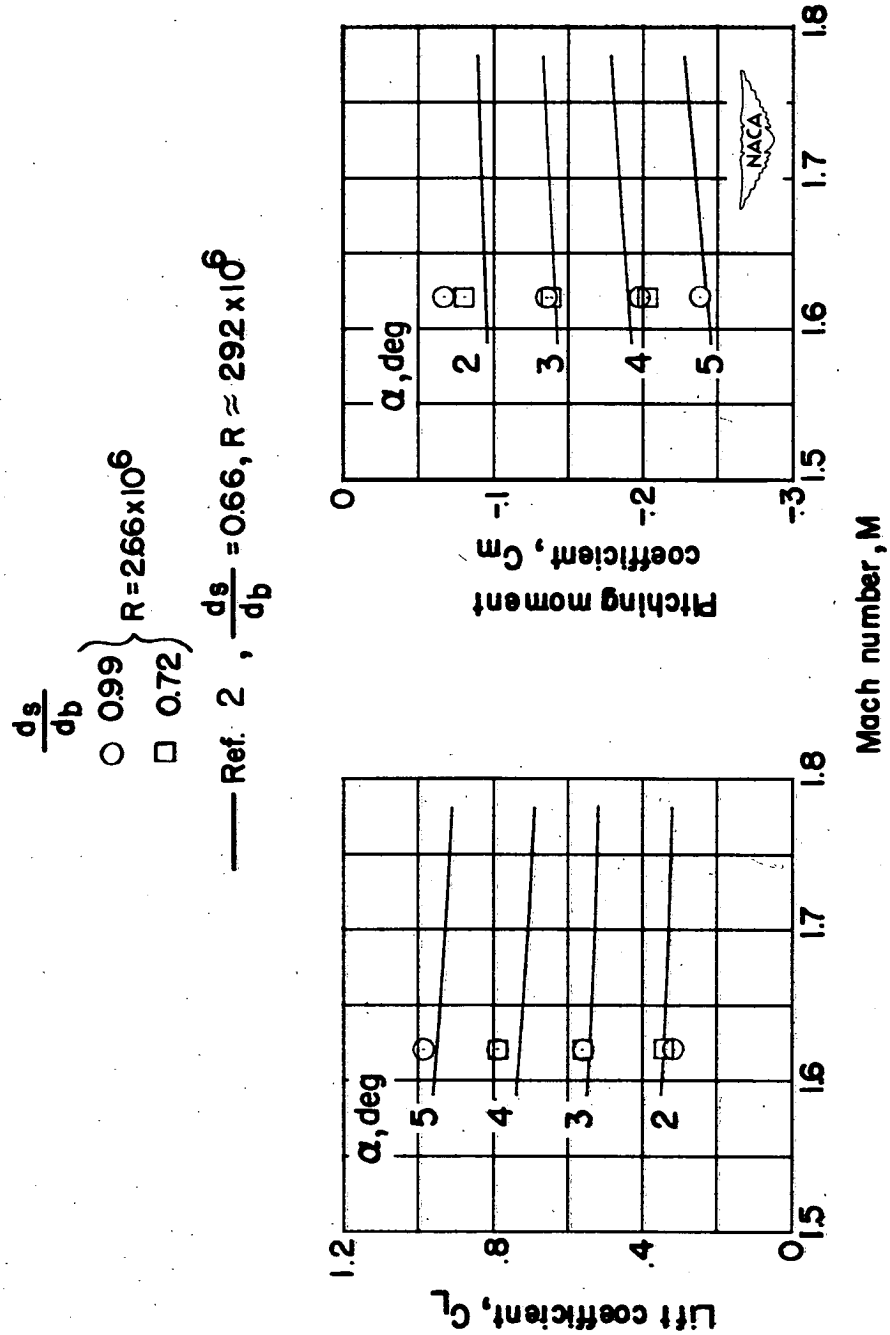

Figure 5.- Comparison of lift and pitching-moment coefficients with results obtained from reference 2.

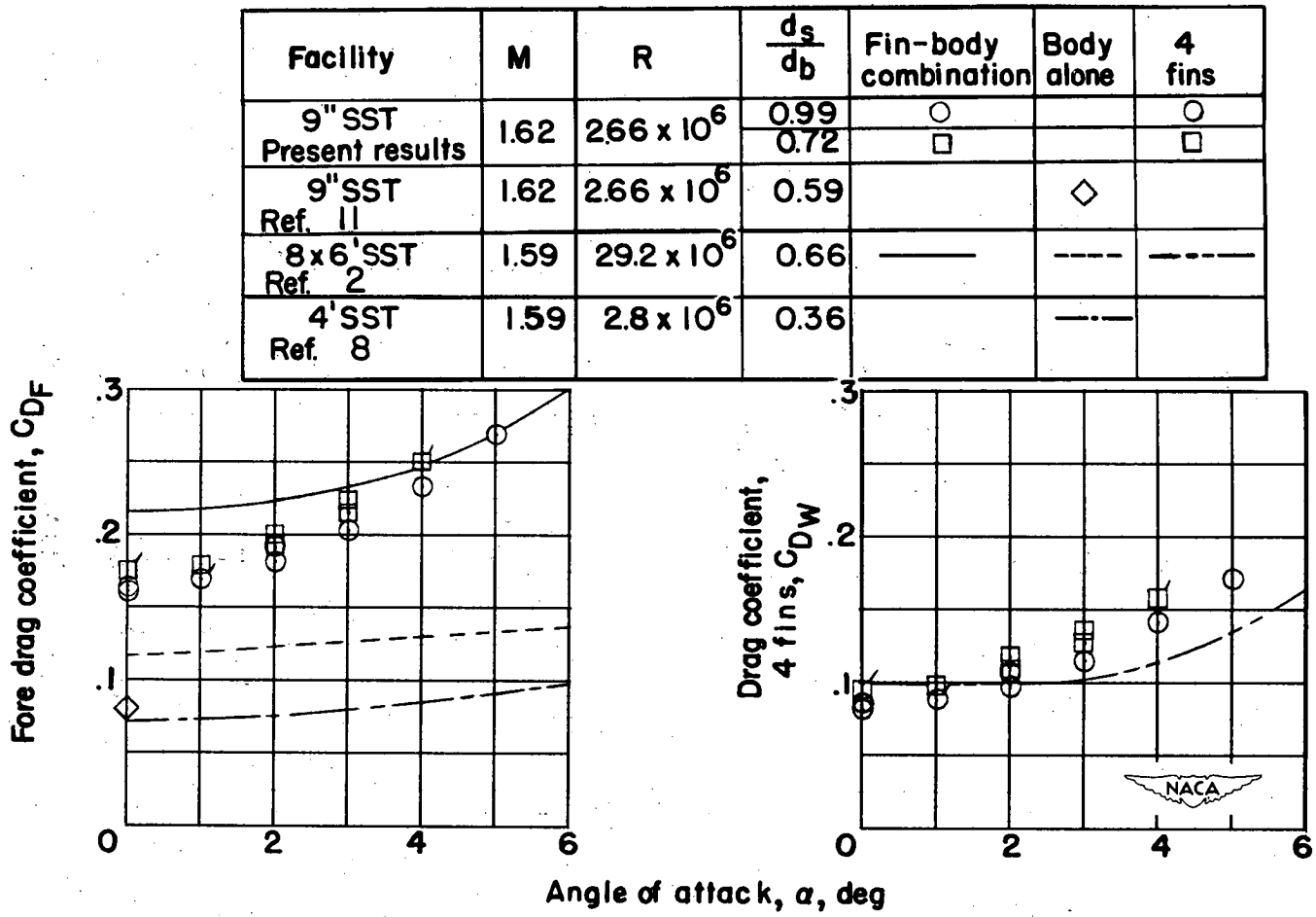

Figure 6.- Comparison of the fore drag coefficients of the body alone, body-fin combination, and fins alone at angles of attack with results obtained from references 2, 8, and 11. Flagged symbols denote check values.

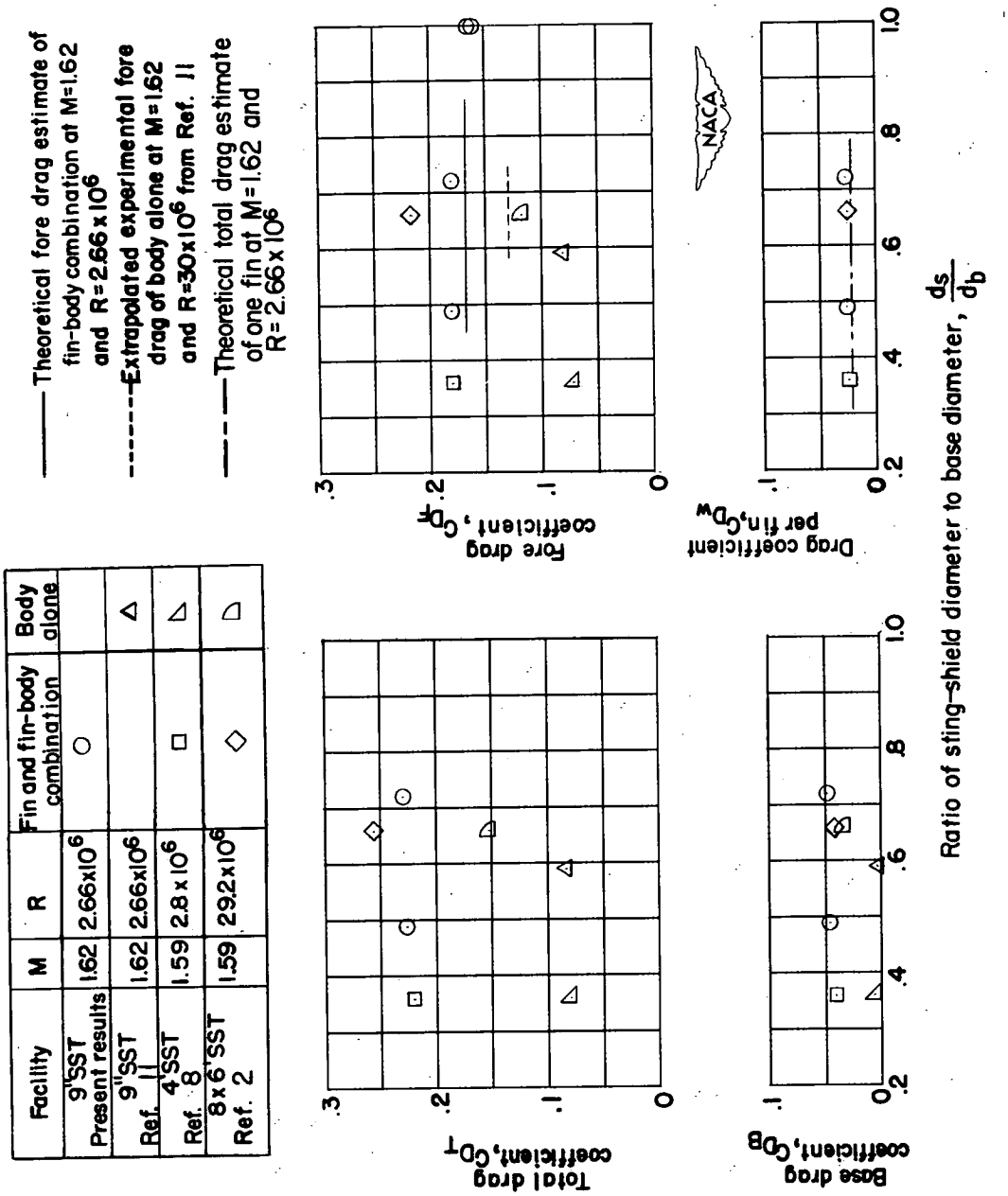

Figure 7.- Variation of the drag coefficients with ratio of sting-shield diameter to base diameter at 0° angle of attack.